Advances in Geo-Energy Research

Vol. 6, No. 3, p. 206-220, 2022

Original article

Characteristics of Precambrian basement intruded by Cretaceous geological intrusions in Monteregian Igneous Province and their impacts on regional thermal structure

Hejuan Liu[1,2]*, Shengnan Ban[1,2], Karine Bédard[3], Bernard Giroux[3]

[1]State Key Laboratory of Geomechanics and Geotechnical Engineering, Institute of Rock and Soil Mechanics, Chinese Academy of Sciences, Wuhan 430071, P. R. China

[2]University of Chinese Academy of Sciences, Beijing 100049, P. R. China

[3]Institut National de la Recherche Scientifique, Centre-Eau Terre Environnement, 490 de la Couronne, Québec G1K 9A9, Canada

Keywords:
Monteregian intrusions
thermal structure
thermal physical properties
fault system

Cited as:
Liu, H., Ban, S., Bédard, K., Giroux, B. Characteristics of Precambrian basement intruded by Cretaceous geological intrusions in Monteregian Igneous Province and their impacts on regional thermal structure. Advances in Geo-Energy Research, 2022, 6(3): 206-220.
https://doi.org/10.46690/ager.2022.03.04

Abstract:
With the progress of geothermal exploration in deep buried geological bodies, high radiogenic geological intrusions have become the hot spot in recent years. However, the assessment of the complex structure, lithology of geological intrusions by the geophysical methods has uncertainty, making it a challenging to accurately predict the thermal structure around the geological intrusions. In southern Québec, Canada, recent studies show that a relative high surface heat flux has been detected in the region enclosed by Montréal, Salaberry-de-Valleyfield and Saint-Jean-sur-Richelieu, around the southwest of the Monteregian Hills, which belong to the Early Cretaceous alkaline and carbonatite intrusions. It is not clear whether these Monteregian intrusions have impacts on the thermal anomaly of the Montréal, Salaberry-de-Valleyfield and Saint-Jean-sur-Richelieu region. The objective of this paper is to numerically investigate the thermal structure in the thermal anomaly region, considering the impact of different Monteregian intrusions. The simplified Monteregian intrusions are embedded into a three-dimensional geological model consisting of the sedimentary formations in the St. Lawrence Lowlands and the simulator Underworld2 is used for the thermal modelling. Simulation results show that the geological intrusions in this region have large impacts on the thermal structure at the local-scale, depending on the radiogenic heat production, thermal conductivity, emplacement depth and size. Temperature in the sedimentary formations may be lower or higher than that of the adjacent geological intrusions, highly depending on the thermal physical characteristics of these intrusions. Furthermore, the complex fault systems also strongly control the thermal distribution in different fault blocks, making the Potsdam Group sandstone located between the Grand-St-Esprit and Notre-Dame-du-Bon-Conseil faults as the potential geothermal reservoir.

1. Introduction

Geothermal energy is an important indigenous energy characterized as clean, renewable, widely distributed, with large reserves and various ways of utilization (Liu et al., 2015). However, compared with other renewable energies, such as wind or photovoltaic energy, its global installed capacity and market share is still very limited. High exploration risk has become one important factor hindering the development of geothermal energy industry. Reservoir temperature and permeability enhancement are the most important factors of a successful geothermal project either in the hot dry rocks (usually in the depth of 3-5 km), or the sedimentary aquifer (Chen et al., 2019; Anyim and Gan, 2020).

For a long period of time, the young, active volcanic or magma related systems, which contribute a very high

*Corresponding author.
E-mail address: hjliu@whrsm.ac.cn (H. Liu); banshengnan21@mails.ucas.ac.cn (S. Ban); karine.bedard@inrs.ete.ca (K. Bédard); Bernard.Giroux@inrs.ca (B. Giroux).
Yandy Scientific Press
2207-9963
Received March 6, 2022; revised April 7, 2022; accepted April 10, 2022; available online April 14, 2022.

temperature at a shallow depth, has become the target of geothermal exploration and exploitation (Capuno et al., 2010). However, in most parts of the world, the geothermal energy with the low to medium enthalpy is the dominant type. In recent years, more potential regions in sedimentary basins with buried high radiogenic geological intrusions and covered by thick sedimentary rocks, are discovered to have thermal anomaly at deep depth, like the Cooper Basin in Australia (Meixner et al., 2012), the Qiongdongnan Basin in China (Tang et al., 2014), and the Serdan-Oriental Basin in Mexico (Lemgruber-Traby et al., 2021).

The surface heat flux, which is the consequence of multiple factors including the radiogenic heat production of rocks, depth of the Moho surface, structural configuration, intrusive events, depth to crystalline basement, fault systems etc., is usually considered to be an efficient indicator for the thermal anomaly at depth (Perry et al., 2010; Jaupart and Mareschal, 2011; Siler et al., 2019; Yang et al., 2020). On a global scale, the average value of heat production is in the range of 0.95-1.20 $\mu W/m^3$ in the upper crust, and 0.4 $\mu W/m^3$ for the lower crust.

Eastern Canada mainly constitutes a great proportion of the Canadian Shield and has always been known as a "cold basin". The Canadian Shield presents an overall low heat flux (i.e., <60 mW/m^2), and the Moho depth of the Grenville Province is around 40 km at depth (Cook et al., 2010). The previous geothermal potential evaluations for the province of Québec have concluded that there is little potential for high-temperature geothermal resources because of the deep buried crustal granitic rocks with low heat generation, high thermal conductivity (>3 W/(m·K)), and low geothermal gradients (Grasby et al., 2012). However, recent evaluations of geothermal potential in parts of the St-Lawrence Platform (especially the Trois-Rivières area), Gaspésie Peninsula, Anticosti Island and Madeleine Islands (Perry et al., 2010; Majorowicz and Minea, 2012, 2013; Liu et al., 2018) have shown that the corrected bottom hole temperatures can reach >120 °C when drilled to the depth of more than 4 km in the sedimentary formations (Bédard et al., 2018), meaning that it still has great potential for geothermal production by applying the double-cycle power generation system or EGS to generate electricity in this region. However, it is unclear about the thermal properties of the Precambrian basement, especially whether this is related with the possible high radiogenic elements in some much younger geological intrusions (e.g., granite, carbonatite etc).

The objective of this paper is to clarify the thermal properties of the Precambrian basement with igneous geological intrusions in the Monteregian Igneous Province (MIP) in Eastern Québec and to study how they affect the regional thermal structure and temperature distribution by numerical modelling. The physical and thermal properties of the Monteregian igneous intrusions are based on literature and experiments. A series of sensitivity analyses have been carried out by thermal modelling in Underworld2 (Quenette et al., 2015), studying the impacts of the heat production generated by radiogenic elements of uranium (U), thorium (Th) and potassium (K), the emplacement depth of igneous intrusions and fault systems on the distribution of regional temperature.

2. Geological setting of the St. Lawrence Platform in eastern Québec

2.1 Tectonic setting

In the southeast of Grenville Province, many dykes, sills, plugs and joints are found, which are parallel to the trend of the Ottawa-Bonnechere graben, considered as a failed arm of a triple junction along the larger Iapetan rift system. It also includes the Ottawa River-Lake Temiskaming and the Saint Lawrence rift systems including Saguenay graben. The age of the dykes along the Ottawa-Bonnechere graben can be dated back to late Precambrian (ca. 575 Ma), representing the initiation time of the rift system. The stratigraphic information indicates that these rift systems were active during the Cambrian period associated with the clastic deposition of the Covey Hill Formation sandstone and conglomerate (Rankin, 1976; Kumarapeli, 1985). The major period of reactivation of faulting within the Ottawa Valley culminated during the Cretaceous Period (145-66 Ma ago) associated with the dominant period of igneous intrusive activity (Bleeker et al., 2011).

The St. Lawrence Lowlands (see Fig. 1), composed of the St. Lawrence Platform and the Anticosti Platform, underwent the initial rifting phase during the latest Proterozoic- Early Cambrian period and convergent phase (from Early Cambrian to Early Ordovician), then evolved into a tectonic active foreland basin, finally ending after the main Taconian accretion event (450-445 Ma) caused by the closure of the Iapetus Ocean (Rimando and Benn, 2005; Lavoie et al., 2009). Afterwards, during Middle to Late Devonian period, Acadian orogeny activated because of the collision of the eastern margin of North America with northwestern part of Africa (Rimando and Benn, 2005), which was followed by the Appalachian orogeny (beginning of Pensylvanian to Later Permian).

2.2 Fault system and stratigraphic sequence

The St. Lawrence Platform is mainly divided into three regions constrained by large basement faults (Fig. 1): 1) the northwest region of the St. Lawrence Platform, which is controlled by the Yamaska fault, is characterized by thin-layered sediments (<750 m in thickness); 2) the intermediate depth basin, with a thickness of 1,250-2,500 m, is located between the Yamaska fault and the Logan thrust fault; 3) a deep basin (with a thickness of more than 2,500 m) is located southeast of the Logan thrust fault which marks the NW margin to allochthonous units (Majorowicz and Minea, 2012). These NE-SW trending normal faults (e.g., Tracy Brook fault, Notre-Dame-du Bon-Conseil fault, Grand-St-Esprit fault, Yamaska fault, Deschambault fault and Delson fault) cut Grenville basement and Lower Palaeozoic sedimentary sequences. Lithostratigraphic units thus thicken and occur at greater depths toward the southeastern direction, and the NWW-SEE trending fault (Bédard et al., 2013a, 2013b).

The St. Lawrence Platform in southern Québec, corresponding to the Cambrian to Early Ordovician passive margin of the Iapetus Ocean, is filled to a depth of ca. 3000 m

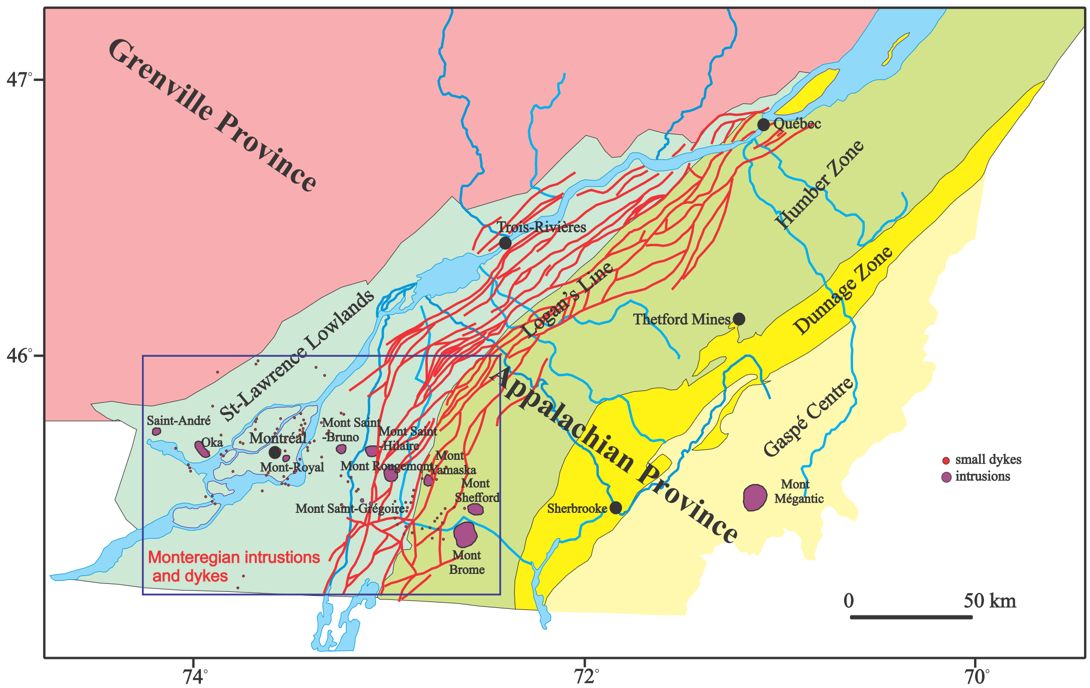

Fig. 1. Location of the St. Lawrence Platform and the intrusions, dykes, faults distribution in the Monteregian Igneous Province (modified after Theriault et al. (2005), blue rectangle shows the scope of MIP).

Table 1. Density, concentration of radiogenic elements and thermal properties of sedimentary rocks in the St. Lawrence Platform.

Groups	Density (kg/m^3)[a]	U (ppm)	Th (ppm)	K (%)	A (μW/m^3)	k (W/(m·K))[a,b]
Potsdam sandstone	2540-2640	0.4-0.45[c]	1.38-1.4[c]	0.05-2.3[c]	0.19-0.42	4.77-6.9
Beekmantown dolomite	2640-2810	0.07-3.08[d]	3-14[d]	0.19-6.26[d]	0.24-2.44	2.7-4.24
TR-BR-Ch limestone	2630-2700	0.2-6.6[d]	2.4-4.7[d]	0.04-2.66[d]	0.22-2.27	2.22-2.98
Utica shale	2700-2710	2.59-3.41[e]	2.9-9.8[e]	0.29-3.42[e]	0.89-1.88	1.93-2.46
SR-LO-QT siltstone	2450-2720	3.1[e]	10.2[e]	0.05-0.8[e]	1.37-1.59	1.91-4.1

Note: a. Nasr et al. (2015); b. Perozzi et al. (2016); c. Rivard et al. (2002) and Owen and Greenough (2008); d. Pinti et al. (2011); e. Vantour et al. (2015).

of Cambrian-Ordovician sedimentary rocks. Based on the deposition sequence, from bottom to top, the sedimentary stratigraphy is mainly composed of 9 groups: Potsdam, Beekmantown, Chazy, Black River, Trenton, Utica, Sainte-Rosalie, Lorraine and Queenston (Liu et al., 2018). The Potsdam group is divided into two formations, the lower Covey Hill Formation is made up of coarse conglomerates, impure fluvial-original sandstones and siltstones and the upper Cairnside Formation is made up of well sorted silica-cemented quartz derived from a marginal marine setting (Lavoie et al., 2009). The Potsdam group and its overlying Beekmantown group show a significant sub-aerial unconformity, where the entire Tremadocian stage is absent. The foreland basin is composed of the Chazy, Black River and Trenton groups, which is filled on a carbonate slope. The rapid, tectonically-controlled, deepening upward event resulted in the deep-sea calcareous shale of the Utica Shale; deep-marine flysch of Lorraine Group and the regressive shallowing upward post-orogenic coarse to fine-grained fluvial to marginal clastics of the Queenston Group (Lavoie et al., 2009).

Rocks from the bottom five groups comprise sandstone for the Potsdam Group with the average porosity and permeability of 3.77%-6.09% and 0.03-0.10 mD, dolomite for the Beekmantown Group with the average porosity and permeability of 1.25%-1.49% and 0.02 mD, and limestone for the Trenton, Black River and Chazy Groups with the average porosity and permeability of 0.88% and 0.01 mD, respectively (Dietrich et al., 2011; Tran Ngoc et al., 2012). Fine-grained siliciclastic rocks of the top four Groups (i.e., Utica, Sainte-Rosalie, Lorraine and Queenston) can be regarded as the good regional caprocks (Majorowicz and Minea, 2012). The density, concentration of radiogenic elements (uranium-U, thorium-Th and potassium-K), calculated heat production and thermal conductivity of these representative sedimentary rocks are listed in Table 1.

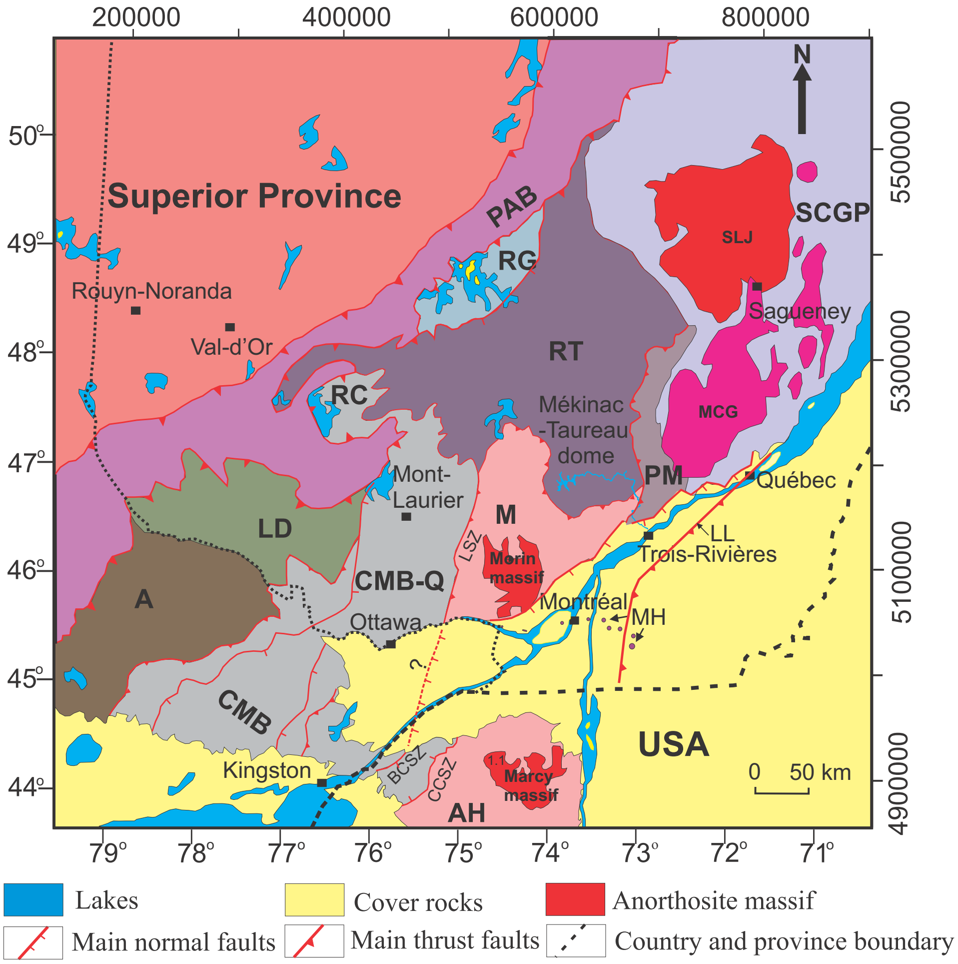

Fig. 2. Main geological regions in Grenville Province, modified from McLelland et al. (2010) and Dufréchou et al. (2014) (A: Algonquin terrane; AH: Adirondack Highlands; CMBQ: Central Metasedimentary Belt of Québec; LD: Lac Dumoine terrane; M: Morin terrane; PAB: Parautochthonous Belt; PM: Porteneuf-Mauricie terrane; RC: Reservoir Cabonga terrane; RG: Reservoir Gouin area; RT: Reservoir Taureau terrane; SCGP: South-Central Grenville Province; SL-A: St. Lawrence platform and Appalachian orogeny; MH: Monteregian Hills; AMCG: Anorthosite-Mangerite-Charnockite-Granite suite; LL: Logan's Line; LSZ).

3. Characteristics of Precambrian basement in western St. Lawrence Platform

The Precambrian basement rocks beneath the St. Lawrence Platform have been studied previously (Liu et al., 2018) considering the Portneuf-Mauricie domain, Morin Terrain, Mekinac Taureau domain and Parc des Laurentides domain. However, the Precambrian Grenvillian basement rocks beneath the western part of the St. Lawrence Platform, especially in Monteregian Igneous Province, are subject to speculation. They may be composed of undifferentiated highly deformed metasedimentary and granulite-grade metavolcanic rocks (Williams, 1991; Guillou et al., 1995; Rimando and Benn, 2005), including marble, biotite gneiss, granitic and anorthosite-mangerite-charnockite-granite (AMCG) suites, etc. To know the thermal property of the Precambrian Grenvillian basement units underlying by the Cambrian-Ordovician sedimentary rocks in the Monteregian Igneous Province, the relationships of different geological terranes in this region should be clarified. The key is to see whether there is tectonic continuity between the Adirondack highlands that is mainly composed of granulite-grade gneisses, and Morin terrane that is mainly composed of a central anorthosite massif, with voluminous mangerite and monzonite, minor jotunite and gabbro, with the host rocks of gneiss at granulite facies including quartzofeldspathic orthogneiss, granitic gneiss and granodioritic gneiss and mafic granulites, amphibolite, politic metasediments and quartzite (Peck, 2012).

3.1 Possible Adirondack-Morin terranes type basement in the Monteregian Igneous Province

The Adirondack highlands terrane is probably a southward extending of the north Morin terrane along Carthage-Colton Shear zone (CCSZ) and Labelle Shear zone (LSZ) (Geraghty et al., 1981). Based on the Nd-model ages of Morin and Adirondack terranes (McLelland et al., 2010), the host rocks of these two terranes are at the same period, i.e., 1.3-1.5 Ga (Fig. 2). They also show similar large anorthosite intrusions

Table 2. Thermal properties of the Precambrian rocks beneath the Morin terrane-St. Lawrence Platform-Adirondack terranes (Souza et al., 2011; SIGEOM database).

Locations	Rock type	N	Th (ppm)	U (ppm)	K (%)	Th/U	k (W/(m·K))[a]
CMB[b]	Bondy complex gneiss	92	0.032-18.85 (3.73)	0.052-5.0 (1.17)	0.05-11.1 (2.5)	0.25-13.3 (2.88)	1.53-5.88 (2.24)
	Granite	25	0.1-57.1 (20.5)	0.4-11.8 (3.7)	0.92-5.57 (4.17)	0.15-44.5 (7.77)	2.76
	Quartzofelspathic gneiss	9	0.4-17 (6.9)	0.4-3.7 (1.5)	0.63-12.84 (4.35)	0.3-13.1 (4.52)	1.53-5.88 (2.24)
	Granitic gneiss	9	0.1-54 (11.0)	0.4-3.5 (1.3)	0.59-6.26 (4.17)	0.25-15.43 (6.05)	1.53-5.88 (2.24)*
	Amphibole	14	0.3-26 (4.2)	0.4-5.6 (1.4)	0.67-5.46 (2.20)	0.84-7.25 (2.92)	2.3
Adirondack[c]	Granodiorite	2	0.26-4.75 (2.29)	0.12-1.2 (0.52)	0.14-1.92 (0.87)	2.27-8.67 (4.66)	3.35-3.92 (3.64)
	Anorthosite	11	0-1.62 (0.28)	0.01-0.84 (0.16)	0-0.96 (0.37)	0-162 (18.5)	1.7-3.78 (2.36)
	Charnockite	6	0.91-18.08 (8.72)	0.5-1.3 (1.00)	1.06-4.94 (3.76)	1.82-13.9 (7.74)	3-3.56 (3.39)
Morin	Quartzite	10	-	1.7-2.4 (2.0)	0.05-0.22 (0.1)	-	6.08-6.38 (6.23)
	Amphibolite	4	11	0.2-1.1 (0.48)	0.91-2.01 (1.46)	-	2.27-2.32 (2.30)
	Granitic, Granodioritic, charnockitic gneiss	18	0.25-26 (6.94)	0.3-3.95 (1.49)	1.48-4.90 (3.73)	0.8-12.4 (4.14)	1.53-5.88 (2.24)

Data source: a. Mareschal database, personal communication, 2017; b. Corriveau (2013); c. Mareschal and Jaupart (2004).

at 1.1 Ga, which was coeval with the Chevreuil suite in the Central Metasedimentary Belt, proving that they may ever behave as a single tectonic entity. Heaumann et al. (2006) also suggested that the Black Creek shear zone (BCSZ) separating the Adirondack Lowlands from the Frontenac terrane and the LSZ may be continuous. Based on the studies of McLelland et al. (2010), the crust of New Jersey-New York-Vermont-Adirondack-Mauricie area connected, which underwent rifting, opening and closing stages with the Central meta-sedimentary belt since ca. 1.4-1.3 Ga. All of these prove that the characteristic of the basement unit underlying the Monteregian Igneous Province may have great similarity with that of Adirondack-Morin terranes (i.e., Central Granulite Belt) (McLelland et al., 2010). Therefore, the averaged Morin-Adirondack type of Grenvillian rocks can be represented as the general Precambrian basement rocks in the Monteregian region.

3.2 The Central Metasedimentary Belt in the Monteregian Igneous Province

It can be inferred from the large scale that the Central Granulite Belt docked with the northeast extending Central Metasedimentary Belt (CMB) connect through the CCSZ and LSZ. During the Elzevirian orogeny (ca. 1.22-1.21 Ga), the accretion of the CMB and Morin terrane to Laurentia (Grenvillian continent-continent collision) was placed, resulting in the over-thickness of the crust during that time. In the southwestern Grenville Geological Province, the outcropped tonalitic Dysart-Redsandstone gneiss in the Central Metasedimentary Belt boundary thrust zone and Mont Holly gneiss complex in the Adirondack Highlands, were thought to the remnants of an early continental rifted arc called the 'Dysart-Mt. Holly arc' at ca. 1.35-1.3 Ga (Agustsson, 2012).

Therefore, the lithology of the basement unit covered by CMB may also represent part of the composition of the thick crustal rocks buried underneath the Adirondack-Morin terranes (i.e., Adirondis in McLelland et al. (2010)). The host rocks of the Central Metasedimentary Belt are mainly composed of marble, quartzite, amphibolite-granulite gneiss complexes, high-grade orthogneiss and paragneiss, granitic to tonalitic gneiss complexes, quartzofelspathic gneiss, aluminous gneiss, sillimanite-quartz gneiss, garnet-biotite-sillimanite gneiss, siliceous gneiss, dioritic gneiss, hornblende gneiss, granitic gneiss, etc (Tremblay et al., 2003). These small terranes comprising CMB (e.g., Central Metasedimentary Belt boundary thrust zone; Harvey-Cardiff domain; Belmont domain; Grimsthorpe domain; Mazinaw domain; Sharbot Lake domain; Frontenac terrane; Adirondack Lowlands) and Adirondack Highlands were formed and subsequently juxtaposed in a complex series of collisional events related to arc formation and amalgamation (Agustsson, 2012), including the Elzevirian and Shawinigan orogenies and two "Grenvillian" events related to later continental collisional orogenic phases: The Ottawan and Rigolet (Rivers, 2008; McLelland et al., 2010; Easton and Kamo, 2011). The thermal properties of the Grenville rocks at the CMB, Adirondack and Morin terrane are collected in detail, shown in Table 2.

4. Geological characteristics of Cretaceous Monteregian intrusions

4.1 Lithology of Monteregian intrusions in the St. Lawrence Platform

During the Cretaceous period, especially 140-100 Ma ago (Eby, 1987), the St. Lawrence Platform, and Appalachian mountains was intruded by a series of intrusive igneous rocks, including dykes, sills, plugs, and fissures (Fig. 1). This was almost coeval with the rifting of the Atlantic-Labrador Ocean, which possibly reactivated some pre-existing faults (Rocher and Tremblay, 2001). At present, the term MH is used to include typical exposed all Cretaceous age intrusions with alkali and carbonatitic affinities from the St. Lawrence Platform to the Appalachian mountains (Gold et al., 1963; Feininger and Goodacre, 1995, 2003). These intrusions were surrounded by shaly materials which acted as an impermeable and easily deformable host rock favouring a dome-shape envelope for the cooling magma mass (Seguin, 1982). It is assumed that, after the Monteregian magmatism, at least 1.6 km of cover rocks were removed by erosion (Clark, 1972).

Table 3. Properties of the Monteregian intrusions.

Intrusions	Longitude W	Latitude N	Outcrop elevation (m)	Outcrop area (km^2)	Average density (kg/m^3)	Distance to basement (km)
St. André	74°18′	45°33′	137	-	-	0
Oka	73°01′	45°30′	65-250	15.8	-	0
Royal	73°36′	45°30′	231	3.51	3155	1.2
Saint-Bruno	73°20′	45°33′	218	4.63	3201	1.8
Saint-Hilaire	73°10′	45°34′	415	9.47	2853	2.6
Saint-Grégoire	73°09′	45°21′	267	0.75	2785	2.8
Rougemont	73°03′	45°29′	384	12.52	3178	3.7
Yamaska	72°52′	45°28′	445	8.44	3144	4.7
Brome	72°38′	45°17′	465	57.93	2775	5.9
Shefford	72°36′	45°22′	526	14.41	2746	6.8
Megantic	71°14′	45°26′	1110	54	2690	≈10.0

Data source: Valiquette and Pouliot, 1977; Seguin, 1982; Eby, 1987; Feininger and Goodacre, 1995, 2003; Roulleau, 2010.

Except for the well-known 11 Monteregian intrusions (St. André, Oka, Mont Royal, Saint-Bruno, Saint-Hilaire, Rougemont, Yamaska, Shefford, Brome and Mégantic), studies of aeromagnetic and gravity also showed the existence of other non-outcropping intrusions, such as the Grand Bois/Iberville pluton and the Boucherville intrusion buried by the Port of Montreal. The studies of the 11 typical intrusions revealed that they differ in the petrology, varying from pyroxenite to peralkaline granite (see Table 3).

From west to east, the chemical composition of these Monteregian intrusions presents a variation trend from mafic or ultramafic rocks to silica-undersaturated, to silica saturated rocks.

1) The westernmost carbonatite complexes at Oka and St. André, are composed of strongly silica-undersaturated rocks and carbonatites, including ijolite, okaites, soviet, rauhaugite, melteigite and urtite. The carbonatite complexes at Oka, containing numerous U-bearing minerals (i.e., apatite, perovskite, pyrochlore and niocalite), show a circular structure, composing of an earlier outer annulus of alkaline silicate-rich rocks and a later central plug of carbonatite (Treiman and Essene, 1985). These carbonatites are often associated with rifts and translithospheric breaks, and they were considered as the partial melting products of mantle materials (Tappe et al., 2008).
2) The central alkaline plutons, including Mont Royal, Saint-Bruno, Saint-Hilaire, Saint-Grégoire, Rougemont and Yamaska, are largely composed of slightly silica-undersaturated (nepheline syenite, essexite) to moderately silica-oversaturated rocks (pyroxenites and gabbros) (Roulleau et al., 2013).
3) The eastern intrusions, including Brome, Shefford and Mégantic, have a large proportion of both felsic rocks and quartz-saturated rocks. The felsic rocks for mounts Brome and Shefford include the series from slightly under-saturated (pulaskite) to slightly over-saturated syenites (nordmarkite). For the easternmost intrusion, i.e., Mégantic, showing also ring structure, is composed of the main minerals of gabbro, diorite, quartz, syenite, nordmarkite, granite etc. The petrography and geochemistry characteristics of this intrusion are very similar to the rocks of the Mesozoic White Mountain intrusions of New England (Bédard, 1985).

4.2 Emplacement stratigraphy of Monteregian intrusions

It seems that very few igneous rocks are exposed and most of other intrusions are entirely capped with Lorraine siltstone (Philpotts, 1970). Except for the Mont Royal intrusion, all other exposed classical Monteregian intrusions were found to be emplaced in the Lorraine siltstone and shale (Fig. 3). Mont Royal intrusion penetrated to the Trenton limestone and the overlying Utica shale. The contact relationships of these igneous rocks and their host rocks show the existence of rheomorphic breccia composed of refractory sedimentary rocks formed from the melting of less refractory beds (Philpotts, 1970). The plutons in the east have penetrated upward with a much greater thickness than those in the west.

4.3 Structure of the Monteregian intrusions

These typical intrusions show great difference in the geometry (Fig. 4). Few geophysical studies of the MH and their surroundings have been published. Based on the observed Bouguer gravity anomalies at the eight classical intrusions (e.g., Mont Royal, Saint-Bruno, Saint-Hilaire, Rougemont, Yamaska, Brome and Shefford), their respective simplified three-dimensional (3D) cylinder (or ring/subcircular) models were computed by Feininger and Goodacre (1995). The tiny Saint-Grégoire was not included in their studies. It can be concluded that the eastern Brome and Shefford intrusions are

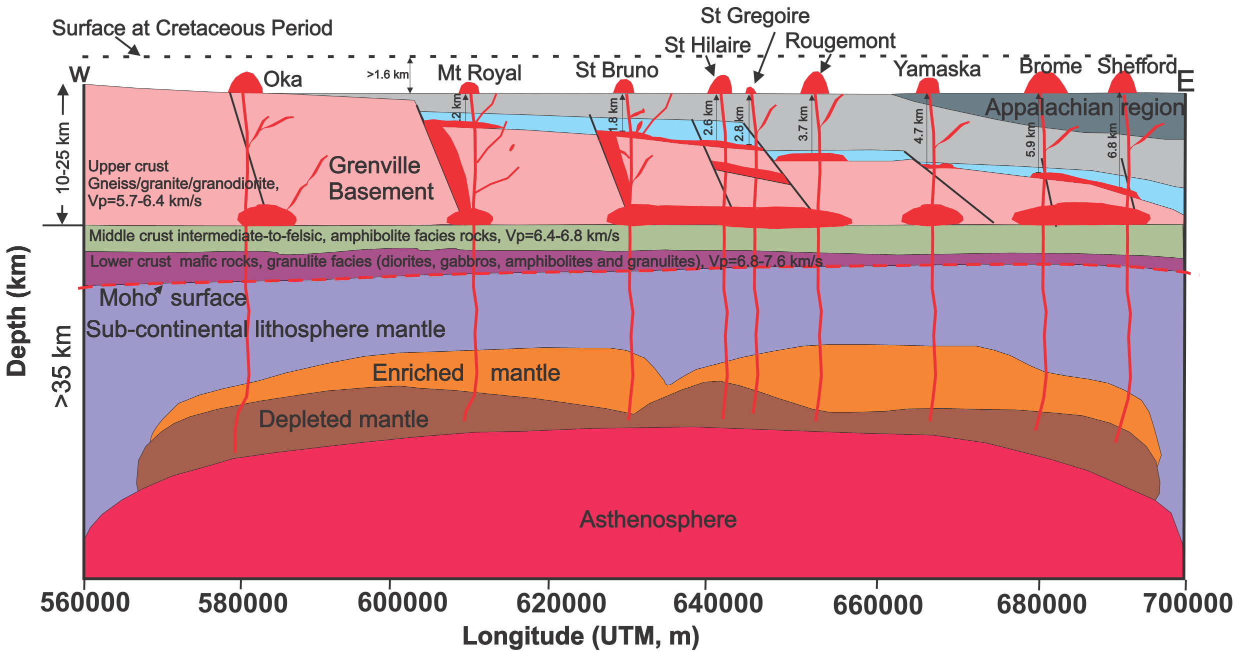

Fig. 3. Schematic diagram of the western-central Monteregian intrusions based on Roulleau et al. (2013) (the top boundary of the mantle is based on Seguin (1982)), the depth of intrusion bodies to the top of basement unit is based on Feiniger and Goodacre (1995), rock types and velocity of P wave for 3 different layers of crust are based on Artemieva (2002).

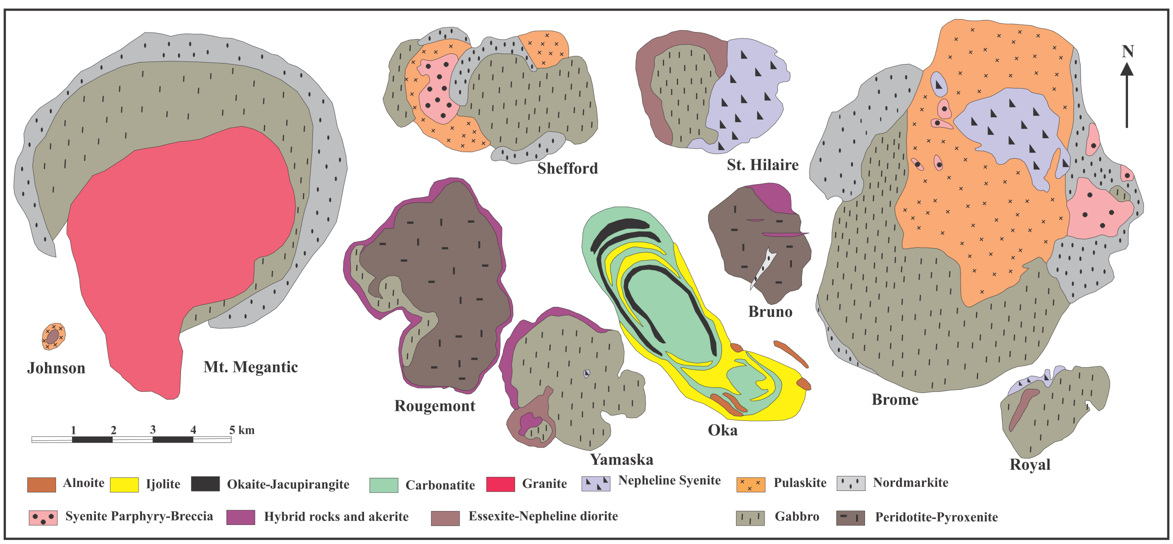

Fig. 4. Surface geometry of classical Monteregian intrusions (modified after Philpotts (1970)).

more slablike, displaying little or no downward enlargement. While for the other 6 intrusions, they are composed of multiple intrusion bodies (i.e., ring-type structure) with downward enlargement trend.

4.4 Genesis of the Monteregian intrusions

These western MH intrusions are located at the interaction of two major paleo-rift systems: Ottawa-Bonnechere graben (may represent a plume-generated Iapetan failed arm that developed at the onset of the breakup of Laurentia and St. Lawrence rift systems, which are composed of a set of Neoproterozoic normal faults associated with the opening of the Iapetus Ocean (Bédard, 1985; Kumarapeli, 1985). About the genesis of the Monteregian intrusions, it is still controversial and there are mainly two types of hypotheses: 1) The hot spot model (Foster and Symons, 1979; Foland et al., 1988) and 2) the continental rift model (Wen et al., 1987; Matton and Jébrak, 2009). For these two models, the hot spot model meets more challenges because of the hotspot track cannot be supported by the age progression (Roulleau, 2010). The appearance of carbonatite intrusions at Oka and St. André and the alkaline Monteregian intrusions along a W to WNW linement at the eastward extension of the Ottawa-Bonnechere graben, may imply that the reactivation of major EW to WNW trending faults during the Cretaceous period in Ottawa-Bonnechere graben (Roulleau, 2010). The St. Lawrence rift system played an important role in the emplacement of the Monteregian intrusions and related numerous dykes, sills (Seguin, 1982; Rimando and Benn, 2005). The easternmost Mt. Megantic pluton located far away from the main axis of Monteregian intrusions, however, may show a different genesis, relating with some major basement faults (Bédard, 1985). Based on these two types of models, the magmas may derive from two types of sources: 1) A deep plume origin (Foland et al., 1988); or 2) the melting of the lithospheric mantle induced by the opening of north Atlantic Ocean (Wen et al., 1987; Roulleau, 2010). It appears in the Monteregian intrusions that two types of magmas with contrasted composition were often alternatively intruding upon the same conduit, thus the thermal plume mechanism is inadequate to support (Seguin, 1982). The mafic to felsic composition changes in the Monteregian intrusions, may reveal the melting of lower crust and the lithospheric mantle, which results in bimodal magmas (i.e., mafic and felsic magma reservoirs). After accumulation to a very large amount, they underplated and intruded into the lower crust (Corriveau and Morin, 2000). During the ascending process of magmas, the host rocks of Monteregian intrusions also underwent different levels of contamination (Seguin, 1982), while Feininger thought that these Monteregian hills or intrusions were sited somewhat at random, in response to the lateral spread of the Monteregian magmas along the Precambrian unconformity and the distribution of local fault systems (Feininger and Goodacre, 1995).

5. Thermal structure and geothermal potential analysis

These MH intrusions cooled down during the Cretaceous period (113-136 Ma) (Feininger and Goodacre, 1995), demonstrating that they may have little or no effect on the present's regional temperature field. However, whether the current fault-controlled deep geothermal system (or circulation) is still affected by the residual heat caused by previous thermal events in or younger than Cretaceous period, through other ways (e.g., radiogenic heat production) is not known. The thermal modelling simulator Underworld developed by Moresi's team was applied by considering the thermal conduction and radiogenic heating effect (Moresi et al., 2007; Quenette et al., 2015; Liu et al., 2018). It is the 3D-parallel geodynamics modeling software based on the programming framework StGermain (Moresi et al., 2007). Within this framework, the Lagrangian Particle-In-Cell Finite Element scheme is used to solve mathematical functions related with specific physical phenomenon, such as thermal convection for a creeping fluid, thermal diffusion, energy, velocity, stress and deformation equations and so on (Rawling et al., 2013).

5.1 Enrichment of the radiogenic elements in Monteregian intrusions

Based on the averaged densities of MH intrusions in Table 3, and the statistical analysis of radiogenic elements (i.e., uranium, thorium and potassium) in some volcanic rocks (e.g., granite, syenite, carbonatite etc) from different sources, see Tables 4 and 5, the radiogenic heat production of different MH intrusions were calculated using empirical function listed in Liu et al. (2018). It shows that the radiogenic heat production of these nine intrusions (i.e., Royal, Saint-Bruno, Saint-Hilaire, Saint-Grégoire, Rougemont, Yamaska, Brome, Shefford, Megantic) is in the range of 0.06 and 8.77 μW/m^3, the carbonatite has even much higher radiogenic heat production up to 29.09 μW/m^3. It implies that the impact of these MH intrusions and some other non-discovered deep buried intrusions are deserved to be investigated in detail, to see the contribution to the regional temperature field.

5.2 Simplified Monteregian intrusions embedded in geological model

In this paper, six simplified Monteregian intrusions (i.e., Royal, St-Bruno, St-Hilaire, Rougemont, Yamaska) are embedded in a 3D faulted geological model in the study region based on drill core information, seismic interpretation and gravity data (Bédard et al., 2013a). The Mont Oka, St. André, Brome, Shefford and Mégantic intrusions are not packed in the 3D geological model because they are out of the study region. This 3D geological model covers 6 groups, including Potsdam, Beekmantown, Chazy-Black River-Trenton and Utica. The depth of the model was extended to 13,250 m to study the impact of different emplacement depths of the Monteregian igneous intrusions on local temperature.

5.3 Boundary conditions

Top boundary: The temperature at the top surface boundary is estimated to be 10 °C, based on the average annual temperature in the St-Lawrence Platform.

Table 4. Radiogenic elements concentration of the carbonatites from the Grenville Province.

Locations	N	Th (ppm)	U (ppm)	K (%)	Th/U	A (μW/m^3)	Data source
Oka intrusions	-	8-137	2-65	-	-	1.19-29.09	Ford et al. (2001)
Outside of the Oka intrusions	-	0.2-13 (4.0)	0.45-1.5 (1.0)	-	-	0.14-1.43	Ford et al. (2001)
CMBbz	5	2.2-29 (9.34)	1.8-4.8 (3.3)	0.025-1.39 (0.92)	1.16-6.04 (2.45)	0.64-3.49	Moecher (1997)
Lorne rapids	4	4-38 (12.5)	13-26 (17)	0.008-0.31 (0.13)	0.15-2.7 (0.86)	4.02-10.38	Mungall (1989)

Note: CMBbz-Central Metasedimentary Belt boundary zone.

Table 5. Radiogenic elements content of the Monteregian intrusions.

Mount	Rock type	N	Th (ppm)	U (ppm)	K (%)	A (μW/m^3)
Royal	Gabbro-pyroxenite	6	7-46 (23.1)	1.93-14.7 (7.1)	0.92-5.76 (3.40)	0.72-8.77
	Gabbro	5	4.17-8.33 (6.33)	1.19-5.34 (2.63)	0.23-0.71 (0.42)	
	Leucogabbro	3	6.9-24.4 (13.2)	1.74-2.12 (1.95)	1.39-2.08 (1.67)	
	Monzonite-quartz monzonite	3	4.7-24 (15.7)	1.22-5.9 (3.66)	0.85-6.73 (3.57)	
	Nepheline diorite	1	9.9	2.4	1.51	
	Essexite	1	9.66	4.79	0.52	
Saint-Bruno	Gabbro-pyroxenite	5	0.6-7.2 (3.82)	0.2-2.2 (0.99)	0.16-0.61 (0.31)	0.13-2.15
	Felsic gabbro	3	7.2-9.4 (8.53)	2.1-3.9 (3.2)	0.15-0.23 (0.18)	
	Peridotite	2	1.6-9.2 (5.4)	0.4-4.4 (2.4)	0.21-0.48 (0.35)	
Saint-Hilaire	Nepheline diorite	3	20.6-24.9 (22.7)	9-11.1 (10.3)	0.54-1.21 (0.9)	4.0-4.95
	Gabbro	3	19.6-22 (21.1)	10-11.8 (11.1)	0.21-0.66 (0.45)	
Saint-Grégoire	Essexite	10	6.8-23.3 (16.8)	1.85-10.4 (6.4)	0.78-2.42 (1.43)	1.05-4.65
	Pulaskite	1	10.5	2.85	2.79	
Rougemont	Gabbro	4	6.9-9.4 (8.4)	2.8-4.5 (4.0)	0.005-0.2 (0.1)	0.70-2.44
	Pyroxene gabbro	1	5.2	0.9	0.008	
	Quartz gabbro	1	10.5	5.1	0.37	
Yamaska	Gabbro	4	0.2-17.7 (10.3)	0.1-6.6 (4.13)	0.12-0.71 (0.86)	0.06-4.59
	Essexite	3	12.8-21 (17.7)	3.11-9.0 (6.50)	0.51-1.85 (1.07)	
	Nepheline syenite	1	14.5	4.4	3.76	
	Akerite	2	9.9-10.1 (10)	2.39-2.53 (2.46)	2.85-3.08 (2.97)	
	Yamaskite	2	0.7-3 (1.85)	0.2-0.7 (0.45)	0.11-0.66 (0.39)	
Brome	Gabbro	9	0.3-32.8 (10.9)	0-21 (6.0)	0.09-0.46 (0.22)	0.03-7.92
	Pulaskite	3	4.8-9.1 (7.0)	1.08-2.1 (1.53)	4.19-5.92 (4.86)	
	Foyalite	2	10-11 (10.5)	2.7	3.29-4.96 (4.13)	
	Nordmarkite	1	4.6	0.96	4.96	
	Nepheline diorite	2	8.2-32.7 (20.5)	2.37-12.7 (7.54)	1.27-1.33 (1.3)	
Shefford	Gabbro	6	15.8-19.3 (17.7)	6.9-10.2 (8.33)	0.43-0.92 (0.66)	2.42-4.11
	Nordmarkite	3	14.6-24.6 (18.3)	3.8-4.87 (4.48)	4.21-4.66 (4.45)	
Megantic	Granite	6	23-33.1 (29.5)	1.4-9.4 (4.74)	3.61-4 (3.81)	0.06-5.06
	Syenite	1	6.5	2	4.86	
	Gabbro	2	0.3-1.2 (0.75)	0.1-0.3 (0.2)	0.19-0.43 (0.31)	
	Diorite	2	1.9-2.3 (2.1)	0.7-0.8 (0.75)	0.75-2.3 (1.53)	

Note: Density of different kinds of rocks are based on the measurement of similar rocks from Paradis (2004).
Data source: Bédard (1985), Eby (1987), Roulleau (2010).

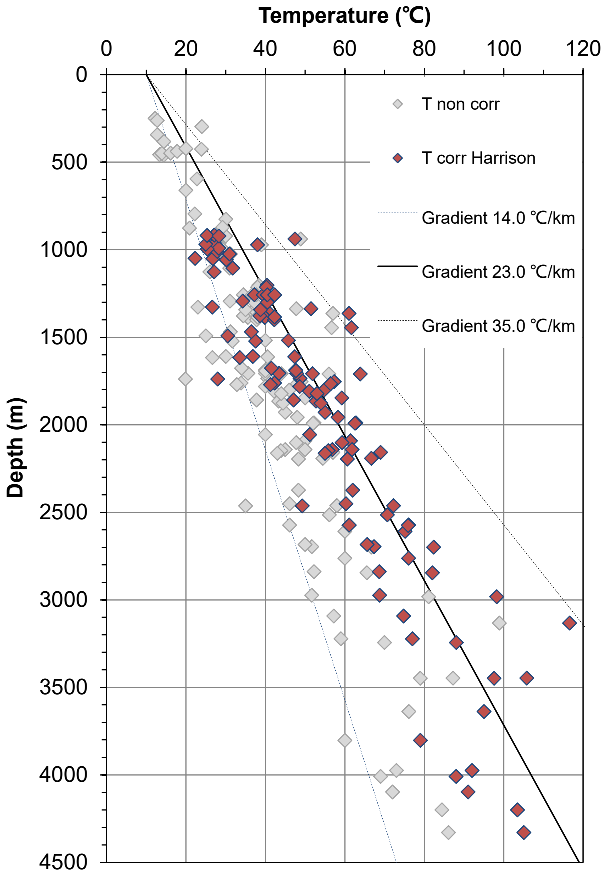

Fig. 5. Relationship between temperature (before and after Harrison correction) and depth in the St. Lawrence Platform.

Bottom boundary: In the thermal modelling, there are often two kinds of thermal boundary (i.e., constant heat flux and constant temperature). In this paper, the temperature at the bottom surface boundary of the 3D numerical model at a depth of 13.25 km is assumed to be 265 °C, based on the average temperature gradient of 19.86 °C/km (Bédard et al., 2013b). However, the temperature data were often measured at the shallow depth, which is difficult to give a clear understanding of the entire basin-scale vertical temperature profile going through the basement. It is also doubtful to apply the interpolation and extrapolation method based on very limited experimental data due to the strong heterogeneity of the rocks. It has a large scope of the geothermal gradient based on available data (19.86-35 °C/km) (Fig. 5), illustrates that much deep temperature measurements together with deep depth drilling are required for a reasonable estimation of temperature gradient.

5.4 Intrusions on local temperature

The initial value of 10 °C is set to the model, based on the thermal properties of the rocks and boundary conditions, Underworld will solve the steady state equation. After the thermal modelling in Underworld, the thermal structure can be generated. To analyze the temperature difference at various depth, the slices of thermal model at different depth were used. The temperature models with and without the consideration of six Monteregian intrusions (from left to right, including Royal, Bruno, Hilaire, Rougemont, Gregoire and Yamaska) were compared. Fig. 6 shows the temperature difference with and without the consideration of geological intrusions, showing that the intrusions have a positive impact on temperature, i.e., higher temperatures are found in the presence of the intrusions. With depth (1, 3, 5 and 7 km), the temperature difference increases, implying the "thermal blanket effect" of heat by sedimentary layers, which is also affected by the relative thermal properties between the intrusions and the surrounding sedimentary layers (Fig. 6).

Temperature perturbation is quite local-scale. When the heat production factor is considered, it shows that the high temperature region concentrates in the high heat production area (Fig. 7(a)), while a relative low temperature region appears when the radiogenic heat production of the intrusion is 100 times lower (Fig. 7(b)), compared with the surrounding sedimentary layers.

5.5 Impact of intrusion depth on local temperature

The intrusion depth also affects the local temperature. When these six Monteregian intrusions were assumed to be emplaced at 5 km depth, it is observed that the temperature difference at 5 km depth will be much larger (Fig. 8(a)) in comparison with the case of emplacement at 13.25 km depth (see Fig. 6). At a 5 km depth, the rocks are dominated by basement rocks with a high thermal conductivity (5.91 W/(m·K)), while the intrusions have a relative low thermal conductivity (2.51 W/(m·K)), the difference in thermal conductivity helps more heat flow from the basement rocks to the geological intrusions. The shallow emplaced intrusions also influence the temperature field at a depth beneath the intrusion bodies. However, at distance far away from the geological intrusive bodies, its disturbance on the temperature can be negligible (Fig. 8(b)).

5.6 Impacts of fault system and geological intrusions on regional thermal structure

In the St. Lawrence Platform, basement faults are highly developed (Bédard et al., 2013a, 2013b). Except for controlling the sedimentation characteristics, normal faults affecting the basement may constrain the thermal structure by controlling the upward or downward movement of structural blocks with different heat production and thermal conductivity. Faults can also significantly influence the hydrogeology and the distribution of the permeability in the reservoir of the geothermal system (Soengkono, 2000; Koestono et al., 2010). By using the 3D geological model with some simplified faults and geological intrusions, their impacts on the distribution of the regional thermal field can be investigated. At the depth of 1 km, the highest temperature concentrates in the block surrounded by Delson, Notre-Dame-du Bon-Conseil, Tracy Brook faults, where the sedimentary rocks in Beekmantown Group have the highest thermal conductivity (i.e., 4.74 W/(m·K). The region bounded by Grand-St Esprit and Deschambault faults also show a relative high temperature feature because it is the

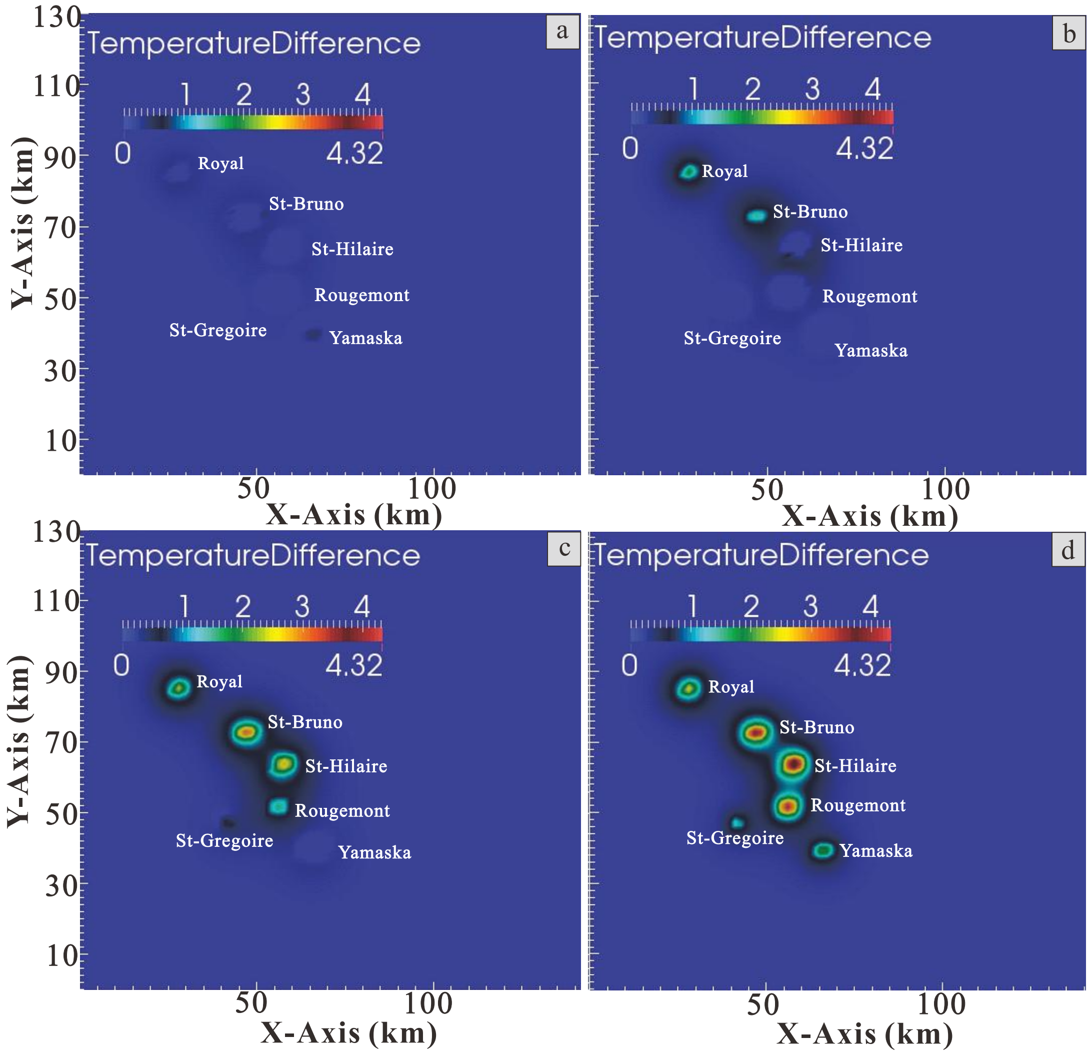

Fig. 6. Impact of simplified Monteregian intrusions on the distribution of local temperature (°C) at different depths (a. 1 km; b. 3 km; c. 5 km; d. 7 km).

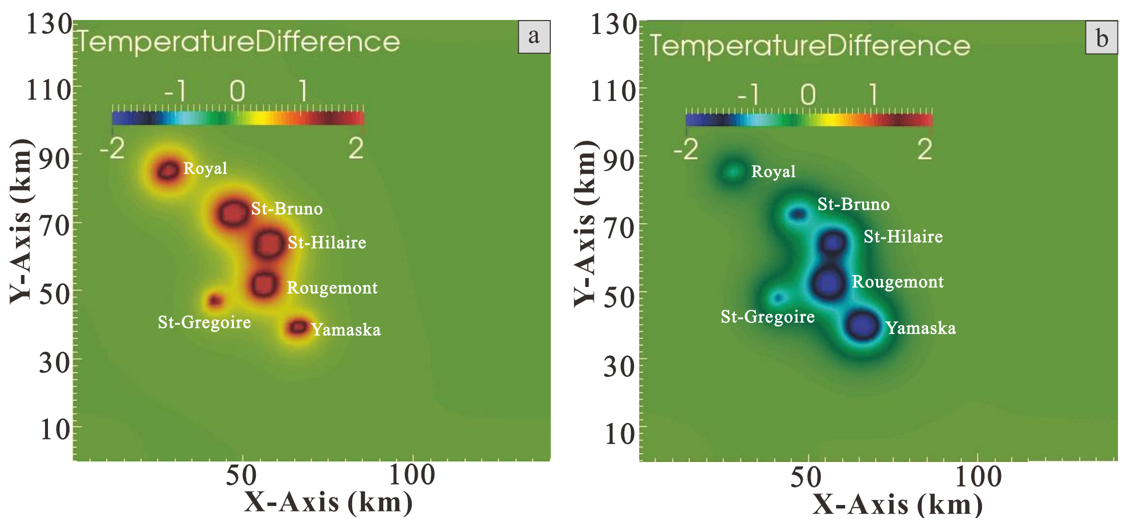

Fig. 7. Impact of radiogenic heat production of the intrusions on the local temperature (°C) at 7 km depth compared with a no intrusion case (a. with the heat production of 3 $\mu W/m^3$; b. with the heat production of 0.03 $\mu W/m^3$).

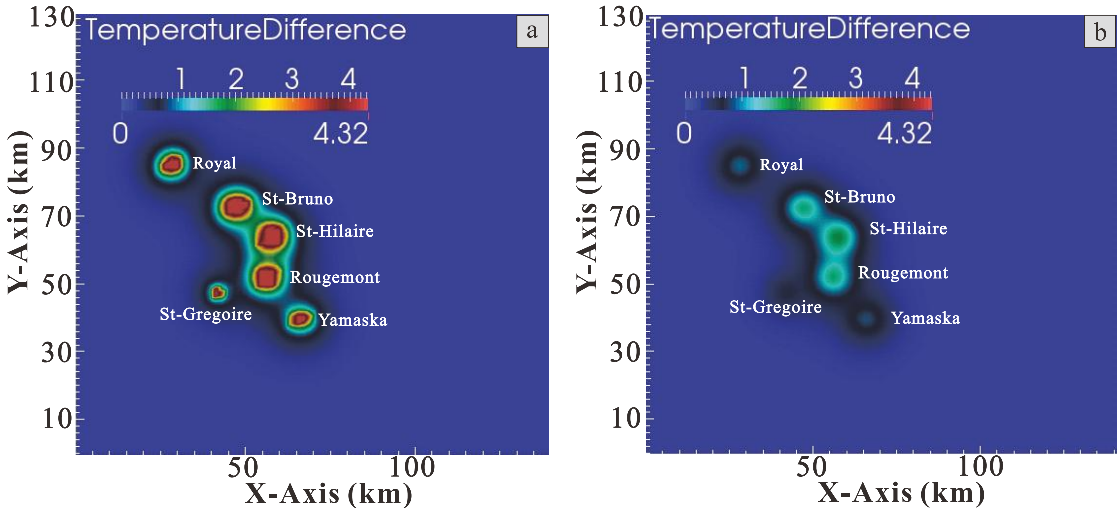

Fig. 8. Temperature difference (°C) contour between the case with the intrusions emplaced at 5 km depth and the case with the intrusions emplaced at 13.25 km depth (depth slice at a. 5 km; b. 10 km).

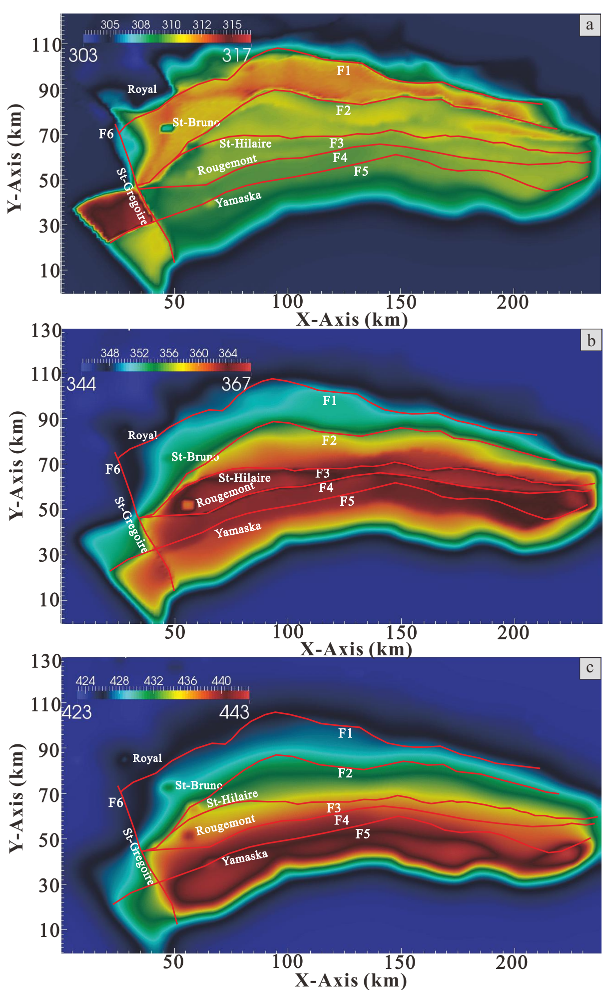

Fig. 9. Temperature (unit: Kelvin) distribution at different depth in the St. Lawrence Lowlands covering the six Monteregian intrusions (a. 1 km ; b. 3 km; c. 7 km; F1: Deschambault fault; F2: Yamaska fault; F3: Grand-St-Esprit fault; F4: Notre-Dame-du Bon-Conseil fault; F5: Tracy Brook fault; F6: Delson fault).

combination of Potsdam and Beekmantown Groups with the top and second highest thermal conductivity (Fig. 9(a)). However, the high temperature region moves and is constrained between Grand-St-Esprit and Tracy Brook faults at the depth of 3 km (Fig. 9(b)). This is due to the dominating effects of the distribution of sedimentary facies, which is characterized by a combination of Potsdam sandstone, Beekmantown dolomite, Utica shale and the caprock. Considering the reservoir properties, the Potsdam Group sandstone can be selected as the target reservoir for extracting hot water or applying a binary cycle power system to generate electricity. At the depth of 7 km, there are only basement rocks and the faults don't extend to this depth. In this case, the high thermal anomaly is located at the south of the Tracy Brook fault (Fig. 9(c)).

6. Conclusions

The geological granitic intrusions emplaced in the sedimentary basins, has attracted the geothermal exploration. In this paper, the characteristics of Monteregian intrusions emplaced at the St-Lawrence Lowland Basin were studied. The deep buried Grenvillian basement beneath the geothermal anomaly region around the Trois-Rivières city was studied based on the geological connection between Morin Terrane, Adirondack Terrane, Central Metasedimentary Belt. Furthermore, both the Grenvillian basement and the Cretaceous Monteregian intrusions were considered in the thermal modeling. The main conclusions can be drawn as follows:

1) The geological intrusions have a considerable impact on the local temperature distribution, depending on the emplacement depth, content of the radiogenic elements, etc. Far away from the intrusion bodies, the impact of temperature disturbance is negligible. The young deep buried intrusions with a large size and much higher

radiogenic element concentrations may have a great contribution to the local thermal anomaly.

2) Sedimentary facies also obviously affect the thermal structure by constraining the distribution of rocks with various thermal properties. Taking the St. Lawrence Platform as an example, the Potsdam Group sandstone located between the Grand-St-Esprit and Notre-Dame-du-Bon-Conseil faults could be selected as the target reservoir for extracting the geothermal fluid.
3) The highly developed fault systems may have a considerable impact on the large-scale hydrothermal convection, which brings the heat to the regions enclosed by Montreal, Salaberry-de-Valleyfield and Saint-Jean-sur-Richelieu. However, this assumption needs further investigations to verify.

This paper can give a better understanding on how the geological intrusions and deep buried basement affect the thermal structure by using the MIP as an example. But more geophysical work is required to confirm the characterization of basement with deep buried geological intrusions. Especially, the heat flow at depth should be better characterize to accurately model the temperatures, as it was shown in Liu et al. (2018) that the bottom boundary condition has a tremendous effect on the modeling results. Furthermore, the complex geometry of these Monteregian intrusions, which show complex thermal properties are difficult to be considered in models, both should be updated with more geophysical work.

Acknowledgement

We acknowledge the financial support from the CAS Pioneer Hundred Talents Program in China (Y826031C01). We would like to thank the reviewers for their constructive comments. We would also like to show our appreciation to Lyal Harris from INRS-ETE for the help of paper revision, Vasile Minea from Hydro-Québec, Jean-Claude Mareschal from University of Montreal, and Daniele Luigi Pinti from University of Québec, who gave us much help during the collection of thermal physical data, to Jennifer Levett from Mira Geoscience Ltd. of Montreal who gave us invaluable help in technical support of GOCAD software, to Prof. Louis Moresi, Steve Quenette, Julian Giordani, Prof. Fabio Capitanio, Jerico Revote, Owen Kaluza and Ben Mather, for the guidance in using the Underworld simulator.

Conflict of interest

The authors declare no competing interest.

References

Agustsson, K. Geochemistry and geochronology of the Central Metasedimentary Belt boundary thrust zone thrust sheets in Southern Ontario, Grenville Province. Bachelor thesis, California, California Polytechnic State University, 2012.

Anyim, K., Gan, Q. Fault zone exploitation in geothermal reservoirs: Production optimization, permeability evolution and induced seismicity. Advances in Geo-Energy Research, 2020, 4(1): 1-12.

Artemieva, I. M. Continental crust, in UNESCO Encyclopedia of Life Support Systems, Oxford, UK, 2002.

Bédard, J. H. The opening of the Atlantic, the Mesozoic New England igneous province, and mechanisms of continental breakup. Tectonophysics, 1985, 113: 209-232.

Bédard, K., Comeau, F. A., Malo, M. Modélisation géologique 3D du basin des Basses-Terres du Saint-Laurent. Final Report INRSCO2-2013-V1.5, 2013a.

Bédard, K., Comeau, F. A., Raymond, J., et al. Geothermal characterization of the St. Lawrence Lowlands sedimentary basin, Québec, Canada. Natural Resources Research, 2018, 27: 479-502.

Bédard, K., Malo, M., Comeau, F. A. CO_2 geological storage in the Province of Québec, Canada-Capacity evaluation of the St. Lawrence Lowlands basin. Energy Procedia, 2013b, 37: 5093-5100.

Bleeker, W., Dix, G. R., Davidson, A., et al. Tectonic evolution and sedimentary record of the Ottawa-Bonnechere graben: Examining the Precambrian and Phanerozoic history of magmatic activity, faulting, and sedimentation. Paper Presented at Field Trip-Excursion 1A, GAC-MAC-SEG-SGA Joint Annual Meeting, Ottawa, 20-24 May, 2011.

Capuno, V. T., Maria, R. B. S., Minguez, E. B. Mak-Ban geothermal field, Philippines: 30 years of commercial operation. Paper Presented at World Geothermal Congress 2010, Bali, Indonesia, 25-29 April, 2010.

Chen, S. C., Ding, B., Gong, L., et al. Comparison of multi-field coupling numerical simulation in hot dry rock thermal exploitation of enhanced geothermal systems. Advances in Geo-Energy Research, 2019, 3(4): 396-409.

Clark, T. H. Région de Montréal: Ministère des Richesses naturelles de Québec. Rapport Géologique, RG-152, 1972.

Cook, F. A., White, D. J., Jones, A. G., et al. How the crust meets the mantle: Lithoprobe perspectives on the Mohorovicic discontinuity and crust-mantle transition. Canadian Journal of Earth Sciences, 2010, 47: 315-351.

Corriveau, L. Architecture de la ceinture métasédimentaire centrale au Québec, Province de Grenville: Un exemple de l'analyse de terrain de métamorphisme élevé. Commission géologique du Canada Bulletin, 2013, 586: 252.

Corriveau, L., Morin, D. Modelling 3D architecture of western Grenville from surface geology, xenoliths, style of magma emplacement, and lithoprobe reflectors. Canadian Journal of Earth Sciences, 2000, 37: 235-251.

Dietrich, J., Lavoie, D., Hanningan, P., et al. Geological setting and resource potential of conventional petroleum plays in Paleozoic basins in eastern Canada. Bulletin of Canadian Petroleum Geology, 2011, 59: 54-84.

Easton, R. S., Kamo, S. L. Harvey-Cardiff domain and its relationship to the Composite Arc Belt, Grenville Province: Insights from U–Pb geochronology and geochemistry. Canadian Journal of Earth Sciences, 2011, 48(2): 347-370.

Eby, G. N. The Monteregian Hills and White Mountain alkaline igneous provinces, eastern North America. Geological Society of London Publications, 1987, 30: 433-447.

Feininger, T., Goodacre, A. K. The eight classical Monteregian hills at depth and the mechanism of their intrusion. Canadian Journal of Earth Sciences, 1995, 32: 1350-1364.

Feininger, T., Goodacre, A. K. The distribution of igneous rocks beneath Mont Mégantic (the easternmost Monteregian) as revealed by gravity. Canadian Journal of Earth Sciences, 2003, 40: 765-773.

Foland, K. A., Jiang, F. C., Gilbbert, L. A., et al. Nd and Sr isotopic signatures of Mesozoic plutons in northeastern North America. Geology, 1988, 16: 684-687.

Ford, K. L., Savard, M., Dessau, J-C., et al. The role of gamma-ray spectrometry in radon risk evaluation: A case history from Oka, Québec. Geoscience Canada, 2001, 28(2): 59-64.

Foster, J., Symons, D. T. A. Defining a paleomagnetic polarity pattern in the Monteregian intrusives. Canadian Journal of Earth Sciences, 1979, 16: 1716-1725.

Grasby, S. E., Allen, D. M., Bell, S., et al. Geothermal energy resource potential of Canada. Canada, Geological Survey of Canada, Open File 6914 (revised), 2012.

Guillou-Frottier, L., Mareschal, J. C., Jaupart, C., et al. Heat flow variations in the Grenville Province, Canada. Earth and Planetary Science Letters, 1995, 13: 447-460.

Jaupart, C., Mareschal, J. C. Heat Generation and Transport in the Earth. Cambridge, UK, Cambridge University Press, 2011.

Koestono, H., Siahaan, E. E., Silaban, M., et al. Geothermal model of the Lahendong geothermal field, Indonesia. Paper Presented at World Geothermal Congress 2010, Bali, Indonesia, 25-29 April, 2010.

Kumarapeli, P. S. Vestiges of Iapetan rifting in the craton of the Northern Appalachians. Geoscience Canada, 1985, 12: 54-59.

Lavoie, D., Pinet, N., Castonguay, S., et al. Hydrocarbon systems in the Paleozoic basins of eastern Canada. Paper Presented at the Calgary 2007 workshop, Geological Survey of Canada Open File 5980, Calgary, Canada, January, 2009.

Lemgruber-Traby, A., Bonte, D., Souque, C. Thermal assessment of Los Humeros geothermal system through basin modeling. Paper Presented at Proceedings World Geothermal Congress, Reykjavik, Iceland, April-October, 2021.

Liu, H. J., Giroux, B., Harris, L., et al. Numerical analysis of the role of radiogenic basement on temperature distribution in the St. Lawrence Lowlands, Québec. Geothermal Energy, 2018, 6: 1-26.

Liu, H. J., Hou, Z. M., Li, X. C., et al. A preliminary site selection system for a CO_2-AGES project and its application in China. Environmental Earth Sciences, 2015, 73: 6855-6870.

Majorowicz, J. A., Minea, V. Geothermal energy potential in the St-Lawrence River area, Québec. Geothermics, 2012, 43: 25-36.

Majorowicz, J. A., Minea, V. Geothermal anomalies in the Gaspésie Peninsula and Madeleine Islands, Québec. GRC Transactions, 2013, 37: 295-300.

Mareschal, J. C., Jaupart, C. Variations of surface heat flow and lithospheric thermal structure beneath the North American craton. Earth and Planetary Science Letters, 2004, 223: 65-77.

Matton, G., Jébrak, M. The Cretaceous Peri-Atlantic alkaline pulse (PAAP): Deep mantle plume origin or shallow lithospheric break-up. Tectonophysics, 2009, 469: 1-12.

McLelland, J. M., Selleck, B. W., Bickford, M. E. Review of the Proterozoic evolution of the Grenville Province, its Adirondack outlier, and the Mesoproterozoic inliers of the Appalachians, in From Rodinia to Pangea: The Lithotectonic Record of the Appalachian Region, edited by R. P. Tollo, M. J. Bartholomew, J. P. Hibbard, et al., Geological Society of America Memoir, pp. 1-29, 2010.

Meixner, A. J., Kirkby, A. L., Lescinsky, D. T., et al. The Cooper Basin 3D map Version 2: Thermal modelling and temperature uncertainty. Geoscience Australia Record, 2012, 60: 1-52.

Moecher, D. P., Anderson, E. D., Cook, C. A., et al. Petrogenesis of metamorphosed carbonatites, Grenville Province, Ontario. Canadian Journal of Earth Sciences, 1997, 34: 1185-1201.

Moresi, L., Quenette, S., Lemiale, V., et al. Computational approaches to studying non-linear dynamics of the crust and mantle. Physics of the Earth and Planetary Interiors, 2007, 163: 69-82.

Mungall, J. A. 1050 Ma pyroxenite-carbonatite suite near Pumbrock, Ontario. Geological Association of Canada-Mineralogical Association of Canada, Program with Abstracts, 1989, 14: A24.

Nasr, M., Raymond, J., Malo, M. Évaluation en laboratoire des caractéristiques thermiques du bassin sédimentaire des basses-terres du Saint Laurent. Paper Presented at of the 68th Canadian geotechnical conference and 7th Canadian permafrost conference, Québec, Canada, 20-23 September, 2015.

Owen, V. J., Greenough, J. D. Influence of Potsdam sandstone on the trace element signatures of some 19th-century American and Canadian glass: Redwood, Redford, Mallorytown, and Como–Hudson. Geoarchaeology, 2008, 23: 587-607.

Peck, W. H. Reconnaissance geochronology and geochemistry of the Mont-Tremblant gneiss of the Morin terrane, Grenville Province, Québec. Geosphere, 2012, 8(6): 1356-1365.

Perozzi, L., Raymond, J., Asselin. S., et al. Simulation géostatistique de la conductivité thermique: Application à une region de la communauté métropolitaine de Montréal. Research Report R1663, Institut National de la Recherche Scientifique-Centre Eau Terre Environnement, 2016.

Perry, C., Rosieanu, C., Mareschal, J. C., et al. Thermal regime of the lithosphere in the Canadian Shield. Canadian Journal of Earth Sciences, 2010, 47: 389-408.

Philpotts, A. R. Mechanism of emplacement of the Monteregian intrusions. Canadian Mineralogy, 1970, 10: 395-410.

Pinti, D. L., Béland-Otis, C., Tremblay, A., et al. Fossil brines preserved in the St-Lawrence Lowlands, Québec, Canada as revealed by their chemistry and noble gas isotopes. Geochimica et Cosmochimica Acta, 2011, 75: 4228-4243.

Quenette, S., Xi, Y. F., Mansour, J., et al. Underworld-GT applied to Guangdong, a tool to explore the geothermal potential of the crust. Journal of Earth Science, 2015, 26(1): 78-88.

Rankin, D. W. Appalachian salients and recesses: Late Precambrian continental break up and the opening of the Iapetus Ocean. Journal of Geophysics Research, 1976, 81: 5605-5619.

Rawling, T. J., Sandiford, M., Beardsmore, G. R., et al. Thermal insulation and geothermal targeting, with specific reference to coal-bearing basins. Australian Journal of Earth Sciences, 2013, 60(8): 817-830.

Rimando, R. E., Benn, K. Evolution of faulting and paleostress field within the Ottawa graben, Canada. Journal of Geodynamics, 2005, 39: 337-360.

Rivard, P., Ollivier, J. P., Ballivy, G. Characterization of the ASR rim: Application to the Potsdam sandstone. Cememt and Concrete Research, 2002, 32: 1259-1267.

Rivers, T. Assembly and preservation of lower, mid, and upper orogenic crust in the Grenville Province-implications for the evolution of large hot long-duration orogens. Precambrian Research, 2008, 16: 237-259.

Rocher, M., Tremblay, A. L'effondrement de la plate-forme du Saint-Laurent: Ouverture de Iapetus ou de l'Atlantique? Apport de la reconstitution des paléocontraintes dans la region de Québec (Canada). Earth and Planetary Sciences, 2001, 333: 171-178.

Roulleau, É. Isotopic tracing of origin and evolution of magmas in the Continental context: Relative contributions of mantle sources and continental crust. PhD thesis, Québec, Université du Québec à Montréal, 2010.

Roulleau, E., Stevenson, R., Polat, A. Geochemical and isotopic (Nd–Sr–Hf–Pb) evidence for a lithospheric mantle source in the formation of the alkaline Monteregian Province (Québec). Canadian Journal of Earth Sciences, 2013, 50(6): 650-666.

Seguin, M. K. Emplacement of the Monteregian hills of Québec, geophysical evidence. Tectonophysics, 1982, 86: 305-317.

Siler, D. L., Faulds, J. E., Hinz, N. H., et al. Three-dimensional geologic mapping to assess geothermal potential: Examples from Nevada and Oregon. Geothermal Energy, 2019, 7: 1-32.

Soengkono, S. Assessment on faults and fractures at the Mokai geothermal field, Taupo volcanic zone, New Zealand. Paper Presented at World Geothermal Congress 2000, Kyushu-Tohoku, Japan, 28 May-10 June, 2000.

Souza, S., Tremblay, A., Ruffet, G., et al. Ophiolite obduction in the Québec Appalachians, Canada — 40Ar/39Ar age constraints and evidence for syn-tectonic erosion and sedimentation. Canadian Journal of Earth Sciences, 2011, 49: 91-110.

Tang, X. Y., Zhang, G. C., Liang, J. S., et al. Modelling of thermal effects of igneous intrusions on the temperature field and organic maturity in the changchang sag, Qiongdongnan basin, South China Sea. Chinese Journal of Geophysics, 2014, 57(2): 219-229. (in Chinese)

Tappe, S., Foley, S., Kjarsgaard, B., et al. Between carbonatite and lamproite—Diamondiferous Torngat ultramafic lamprophyres formed by carbonate-fluxed melting of cratonic MARID-type metasomes. Geochimica et Cosmochimica Acta, 2008, 72: 3258-3286.

Theriault, R., Laliberte, J. Y., Brisebois, D., et al. Fingerprinting of the Ottawa-Bonnechere and Saguenay grabens under the Saint-Lawrence Lowlands and Québec Appalachians: Prime targets for hydrocarbon exploration. Paper Presented at the Geological Association of Canada, Annual Conference, Halifax, Nova Scotia, 16-18 May, 2005.

Tran Ngoc, T. D., Konstantinovskaya, E., Lefebvre, R., et al. Caractérisation hydrogéologique et pétrophysique des aquifères salins profonds de la région de Bécancour pour leur potentiel de séquestration géologique du CO_2. Institut national de la recherche scientifique-Centre Eau T erre Environnement, INRSCO2-2011-V2.6, Québec, 2012.

Treiman, A. H., Essene, E. J. The Oka carbonatite complex, Québec: Geology and evidence for silicate–carbonate liquid immiscibility. American Mineralogist, 1985, 70: 1101-1113.

Tremblay, A., Long, B., Massé, M. Supracrustal faults of the St. Lawrence rift system, Québec: Kinematics and geometry as revealed by field mapping and marine seismic reflection data. Tectonophysics, 2003, 369: 231-252.

Valiquette, G., Pouliot, G. Geology of Mounts Brome and Shefford. Ministére des Richesses naturelles du Québec. E.S. 1977.

Wen, J., Bell, K., Blenkinsop, J. Nd and Sr isotope systematics of the Oka complex, Québec, and their bearing on the evolution of the sub-continental upper mantle. Contributions to Mineraloy and Petrology, 1987, 97: 433-437.

Williams, D. A. Paleozoic geology of the Ottawa-St. Lawrence Lowland, southern Ontario. Ontario Geological Survey, 1991, 116: 107-110.

Yang, W. B., Han, S. B., Li, W. Geological factors controlling deep geothermal anomalies in the Qianjiaying Mine, China. International Journal of Mining Science and Technology, 2020, 30: 839-847.